Crimson Publishers
Wings to the Research

Research Article

Geopolymer Cement Based on Bioactive Egg Shell Waste or Commercial Calcium Carbonates

HHM Darweesh*

Refractories, Ceramics and Building Materials Department, National Research Centre, Egypt

ISSN: 2576-8840

***Corresponding author:** HHM Darweesh, Refractories, Ceramics and Building Materials Department, National Research Centre, Cairo, Egypt

Submission: March 30, 2022

Published: April 19, 2022

Volume 17 - Issue 1

How to cite this article: HHM Darweesh*. Geopolymer Cement Based on Bioactive Egg Shell Waste or Commercial Calcium Carbonates. Res Dev Material Sci. 17(1). RDMS.000901. 2022.
DOI: 10.31031/RDMS.2022.17.000901

Abstract

Geopolymer cements were prepared using a bioactive waste like Egg Shell Powder (ESP) and Commercial Calcium Carbonate (CCC). These geopolymer cements were prepared by adding 6M phosphoric acid as a chemical hardener to siliceous clay containing 0, 3, 6, 9, 12 and 15wt. % from ESP and CCC. Results showed that Toshka clay (T-C) which is siliceous material, and it is mainly composed of kaolinite, illite and quartz phases. This was confirmed by the XRD patterns, and other trace minerals have also been found. The ESP is composed of calcium carbonate, $CaCO_3$. Results showed that the bulk density of the prepared geopolymer cements improved and increased with the gradual replacement with ESP or CCC at the expense of the T-C only up till 12wt. %, while the water absorption and apparent porosity decreased, whereas the flexural and compressive strengths improved and enhanced. However, all the characteristics of geopolymer cements based on ESP are higher than those based on CCC. The optimum geopolymer cement was that incorporated 12wt. % ESP waste because it achieved the best results. It was also concluded that the low-grade calcium carbonate-rich wastes of the egg shells could be used as a pore-forming agent to produce porous geopolymer cements. This could be successfully utilized as thermal insulation units if the geopolymer cement incorporated high amounts of it.

Keywords: Geopolymer; Clay; Egg shell; Hardener; Density; Porosity; Strength

Introduction

Scope of the problem

Geopolymer is a semi-crystalline aluminosilicate material with a three-dimensional network, which was firstly used by Davidovits [1]. It could be prepared by mixing an aluminosilicate powder with an activating hardener [2]. The activating hardener was applied as water glass (Na_2SiO_3 or K_2SiO_3), and phosphoric acid (H_3PO_4) [2-5]. Several studies have been done on the synthesis of porous geopolymer cements, which used in many applications in eco-construction [6], adsorption [7,8], catalysis [9], water absorption and many others [10,11]. This type of cements is similarly synthesized as those with no pores, but only a pore-forming agent whether a powder or a solution must add to the aluminosilicate material. These pore-forming agents that are used in an alkaline medium are aluminum powder [12,13], silica fume [14], hydrogen peroxide [2,15-17], sodium perborate -----etc. [18], which are very expensive. Also, metakaolin could be used as a source of aluminosilicate to produce porous materials. Geopolyms synthesized from metakaolin often have properties similar to those obtained from volcanic slag. This is contributed to the low reactivity of volcanic slag if compared to those of metakaolin. The low reactivity of volcanic slag is due to its low specific surface area when compared to that of metakaolin [19].

Recycling of natural bio/wastes, e.g. chicken or generally birds eggshells, oyster shells, snail shells and/or agro/wastes, e.g. rice husk ash [20], wheat stalk ash [21], sun flower ash [22], sugarcane bagasse ash [23], saw dust ash [24], coir pith ash [25], Physalis pith ash [26], glass waste powder [27], limestone waste powder [28], etc. offers many economic and environmental benefits, as it helps to reduce disposal costs in landfills and maintain a healthy environment. Though these eggshells have a high content of $CaCO_3$, until today it is not yet used as a pore-forming agent for the production of porous geopolymer materials in acidic and/or alkaline media hardeners or activators. Geopolymeric materials are often characterized by its low thermal conductivity, low compressive strength and low bulk density [29,30]. The blowing agents which commonly used for the production of porous geopolymer cements are aluminum powder [29-31], hydrogen peroxide [2,32], silica fume [33], sodium perborate [18,34] when used waste glass powders to prepare porous geopolymers using eggshell powders as a source of $CaCO_3$ [35,36]. Also, porous geopolymeric cements based on phosphoric acid were prepared using limestone as a pore-forming agent.

Goals of the study

The main goal of the present work is to prepare geopolymer cements from a siliceous clay incorporating a bioactive waste material as eggshell powder and comparing with those obtained by using commercial calcium carbonates $CaCO_3$. The physical and mechanical properties were investigated.

Experimental

Raw materials

The raw materials used in this study are clay (T-C), Commercial Calcium Carbonate (CCC), commercial Phosphoric Acid (PA) and Bio-Calcium Carbonate (BCC) which was taken from chicken eggshells. A representative clay sample of Dakhla Formation from Tushka region at South Western Desert, Egypt was used in this work as the main raw material. The Stratigraphic units, representing the rock outcrops in Wadi Kurkur area from the base to top are Nubia, Dakhla, Kurkur, Garra, Dungul Formations and quaternary deposits [37,38]. Following the deposition of Nubia Formation, marine conditions prevailed, which are resulting in the deposition of shale with a little sandstone and carbonate intercalations during Maastrichtion time (the Dakhla Formation [39]. At Wadi Kurkur, the Dakhla Formation crops out with a variable thickness, reaching its maximum at the latitude 23° 57¯N and longitude 32° 23¯E (Map 1). It appears like a wall formation, composed of about 5 m thick compact grayish-green shale with discontinuous cracked bed at the base, followed by ferruginous thin bands intercalated with siltstone bands. This is followed by other 10m thick fossile greenish gray shale with alternated siltstone layers at the top [40].

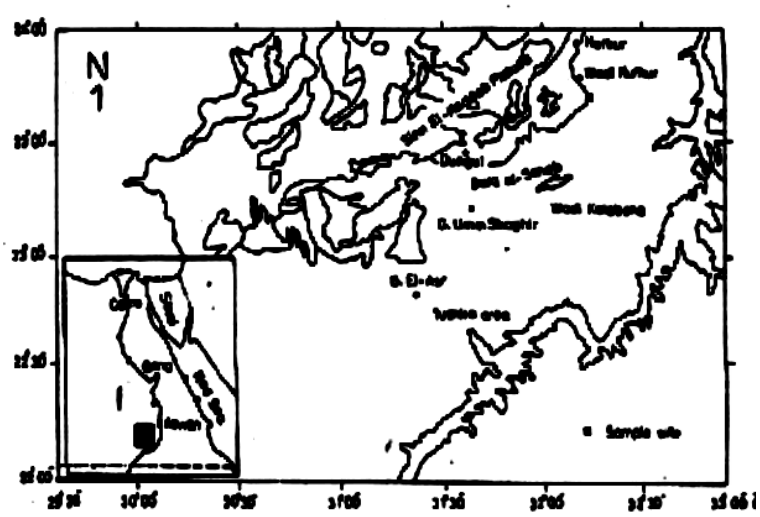

Map 1: Location map (After Awad, 2003).

The clay sample (TC) was taken from Toshka region. Toshka region is located on latitude 20° 30¯N and longitude 31° 53¯E at 250km south of Aswan which was related to the Upper Cretaceous age [41]. About 30kg clay was collected from the 85thkm north of Aswan/Abu-sumple asphaltic road (Map 1). It is a dark yellowish grey. The clay sample was crushed, ground and quartered to have a representative sample, which was well ground to pass a B.S. 100 mesh sieve. The chemical analysis of the T-clay sample as performed with X-ray florescence technique (XRF) is SiO_2, 48.74%, Al_2O_3 17.72%, Fe_2O_3 10.86 %, CaO 1.11%, MgO 1.99%, Na_2O 1.08 %, K_2O 0.97 %, TiO_2 1.85 %, P_2O_5 0.21 %, Cr_2O_3 0.02 %. Hence, the major components of clay sample are silica (48.74%), alumina (17.72%) and iron oxide (10.86%) in addition to ~7.0% of other minor oxides. This means that the total fluxing oxides of the clay sample is ~18.0%. The TC sample was calcined up to 850 °C for two hours soaking time in a suitable furnace before its using. The shells were collected from a local plant in Beni Suef, Egypt. These shells were first well-washed with tap water several times to remove the organic content. Then, it

lets to dry in the open air for 4 hours directly under the sun shine. After that, the shells were manually broken into small pieces (about 1-3mm). The broken shells had fired up to 500 °C in a suitable electrical oven for 2 hours soaking time with a heating rate of 10 °C/min. Then, the calcined shells were well ground using a ball mill to obtain the very fine shell powder. This powder was sieved till the full passage through 80μm mesh sieve. The CCC and PA were supplied by El-Gomhoria chemical company, Ramsis street, Egypt (Figure 1).

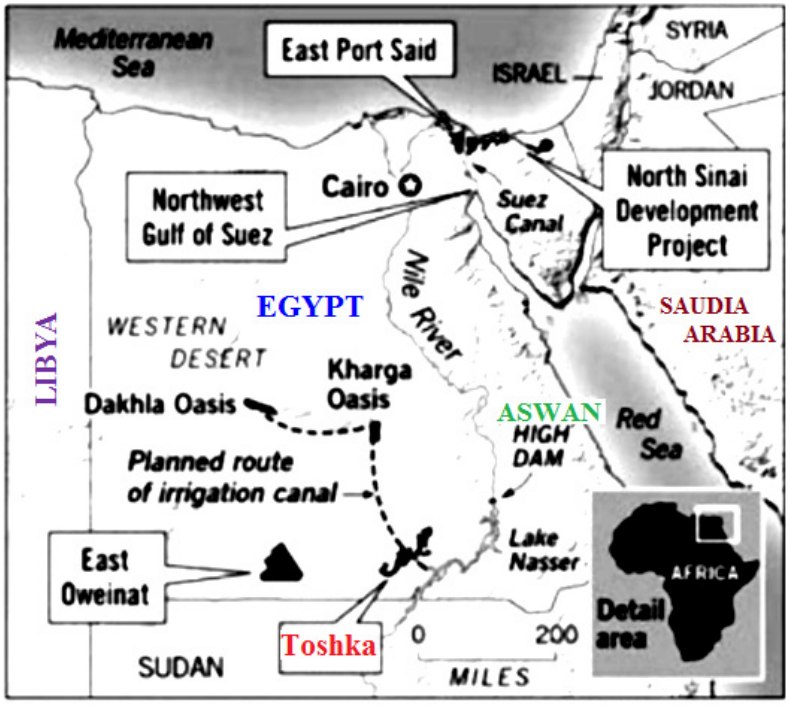

Figure 1: Location of Toshka area from which the clay sample was taken.

Preparation of the hardener

The hardener was prepared by diluting the commercial solution of phosphoric acid (H_3PO_4, 85% purity) in distilled water to obtain 6M concentration solution. The prepared hardener was left at room temperature before use for 24 hours [42-46].

Geopolymer cement production process

The fresh geopolymer cement batches were prepared by gradually substituted with the two types of carbonates (CCC and BCC) containing 0, 5, 10 and 15wt. %. Therefore, there are two groups according to the type of carbonate. The first group was containing 50wt. % T-clay and 50wt.% commercial $CaCO_3$, and the bio-carbonates (BCC) was substituted at the expense of CCC. The second group was containing 50wt. % T-clay and 50wt. % boi-$CaCO_3$ (BCC), which was substituted by CCC. Table 1 shows the batch composition of the two groups. These batches were manually mixed for three minutes and then mixed mechanically in a suitable mixer for another three minutes. The hardener solution was gradually added to the previously calcined clay (metakaolin). The liquid to solid mass ratio was maintained at 0.83. Hence, the various formulations were then mixed manually for 5 minutes. The geopolymer cement pastes were molded into cubic stainless-steel molds (2.5 x 2.5 x 2.5cm^3). The test pieces were then placed in a suitable lab. oven at 65 °C for 24 hours to accelerate the polycondensation process. The obtained geopolymer cement are then demolded, sealed in plastics and left at room temperature (25±1 °C) and a relative humidity of (55±5%) for 28 days.

Table 1: Batch composition of the two groups containing wates of BCC and CCC, wt. %.

Group Material	G0	G1	G2	G3	G4	G5
BCC	0	3	6	9	12	15
CCC	0	3	6	9	12	15

The water absorption, Bulk Density (BD) and apparent porosity (%) of the hardened geopolymer pastes [47-51] were calculated from the following equations:

$$W.A, \% = (W1 - W2)/(W3) \times 100 \quad (1)$$

$$B.D, (g/cm^3) = W3 / (W1-W2) \quad (2)$$

$$A.P, \% = (W1 - W3) / (W1-W2) \times 100 \quad (3)$$

Where, W1, W2 and W3 are the saturated, suspended and dry weights, respectively. Rod-shaped samples of 1x1x7cm^3 dimensions were cast for Flexural Strength (FS) where it could be carried out using a simple beam with three points loading system (Figure 2). The strengths were determined with a hydraulic press. The determination of the flexural strength was carried out by uniform load-

ing at speeds of (50±10) N/s, while the compressive strength was determined by uniform loading at a rate of (2400 ± 200) N/s [51]. The FS [52-54] could be measured due to the following relation:

$$FS, MPa = 3 (L \times S) / 2 (W \times T^2) / 10.2 \quad (4)$$

Where, FS is the flexural strength, MPa, L is the beam or loading of rupture, kg, S is the Span (distance between the two lower beams, 5cm), W and T are the width and thickness of samples, cm.

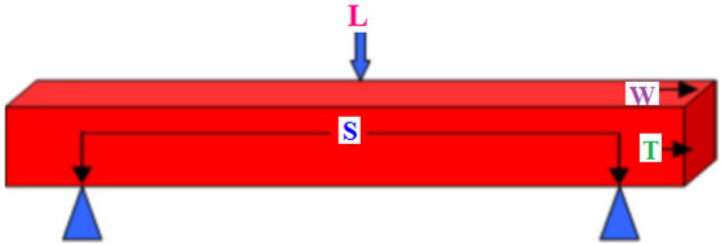

Figure 2: Schematic diagram of the bending strength, L: load, S: spam, T: thickness, W: width.

The compressive strength (CS) of the various hardened cement pastes [54-57] was measured and calculated from the following relation:

$$CS = L (KN)/Sa (cm^2) KN/m^2 \times 102 (Kg/cm^2)/10.2 (MPa) \quad (5)$$

Where, CS is the compressive strength (MPa), L is the load taken (Kg), Sa is the surface area. Thereafter, about 10 grams of the broken specimens were first well ground, dried at 105 **ºC** for 30min. and then were placed in a solution mixture of 1:1 methanol: acetone to stop the hydration [58-60].

The XRD analysis was achieved by a Phillips X-ray diffractometer (XRD), PW 1710 powder with an anticathode copper radiation and Cu-Kα radiation, wave length of 1.54178 Å and a graphite monochromator. The tube working voltage was 40kV and current strength was 30mA, in the range 5-50° 2θ with a step of 0.02 and 0.5 seconds retention time for each step. The DTA-TGA analysis was carried out using NETZSCH Geratobau Selb, Bestell-Nr. 348472c at a heating rate 10 °C/min up to 1000 °C. The fourier transform infrared spectra (FT-IR) were performed by Pye-Unicum SP-1100 in the range of 4000-400 cm^{-1} and a resolution of 500cm^{-1}. The particle size distribution (PSD), X-ray fluorescence (XRF), X-ray diffraction (XRD) patterns and DTA-TGA analyses were carried out in the Metals Institute, El-Tabbine, Cairo, Egypt. The FT-IR analysis was done in the National Research Centre, Dokki, Cairo, Egypt [61].

Results and Discussion

Characterization of clay and eggshell samples

Table 2: Particle size distribution of the T-clay and eggshell samples, µm.

Materials	Particle Size Distribution, µm					
Size	>63	63-16	16-8	8-2	<2	Total
T-Clay	1.43	1.68	2.96	9.14	84.79	100
Eggshell	0.12	0.16	0.18	1.31	98.23	100

Table 2 shows the particle size distribution of the T-clay and eggshell powder samples, respectively. The T-clay sample contains about 0.06% gravel, 32.58% sand, and 8.25 % silt and 59.11% clay. The eggshell contains about 98.23wt. % very fine particles. Results of analysis proved that the T-clay sample has a very wide granulometry because its uniformity coefficient is greater than 200. Hence, it is siliceous clay with a few silts and nearly with no gravel [62].

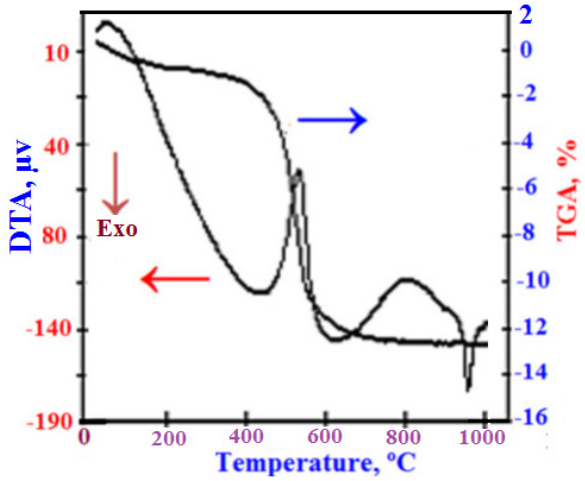

Figure 3: The DTA-TGA thermograms of the T-clay sample.

The T-clay sample was characterized by the DTA-TGA thermograms, while that of the eggshell was by XRD patterns and FT-IR spectra. Figure 3 illustrates the DTA-TGA thermographs of the used T-clay sample. The endothermic peak at the temperature range 100-400 °C is due to the evaporation or dewatering of the free or hygroscopic water, absorbed and/or structural water. The endothermic peak at the temperature range of 750-900 °C is due to the calcination of limestone. The endothermic peak at the temperature range 500-760 °C is contributed to the conversion of kaolinite phase (Al_2O_3. $2SiO_2$.$2H_2O$ or AS_2H2) to metakaolin phase (Al_2O_3.$2SiO_2$ or AS_2), which in turn is converted to mullite phase ($3Al_2O_3$.$2SiO_2$ or A_3S_2) at 980-1000 °C [60,61].

Figure 4 illustrates the X-ray diffraction patterns (XRD) of the T-clay and eggshell powder samples. It indicates that all of the characteristic peaks of calcite ($CaCO_3$) were detected in the eggshell sample, i.e. the eggshells are mainly composed of natural calcium carbonates [62-64], while the T-clay sample is essentially composed of kaoline, quartz, illite and gibbsite.

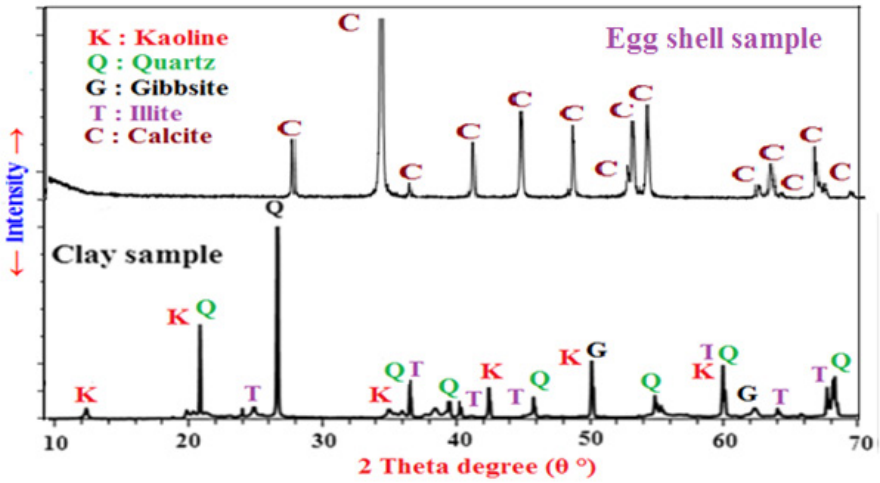

Figure 4: XRD patterns of the T-clay and eggshell powder samples.

Figure 5 shows the FT-IR spectra of the eggshell powder sample. The weak absorption bands at the temperature range of 1660-16750cm^{-1} and 3500-3650cm^{-1} are attributed to the dewatering or evaporation of free water and decomposition of combined water, respectively indicating the OH^- or H-O-H bonds of water molecules [65]. Also, the bands at 782, 2518, 2877, 2985cm^{-1} are assigned to stretching vibration modes of C=O bonds of carbonate groups [61], while those at 713, 875 and 1419cm^{-1} are attributed to the vibrations bands of the CO bonds of calcite. The bands at 1154 and 673cm^{-1} are essentially contributed to the CO_3^{2-} ions [61]. The stretching band at 597cm^{-1} is mainly assigned to the O-Ca-O and Ca-O bonds [61,63].

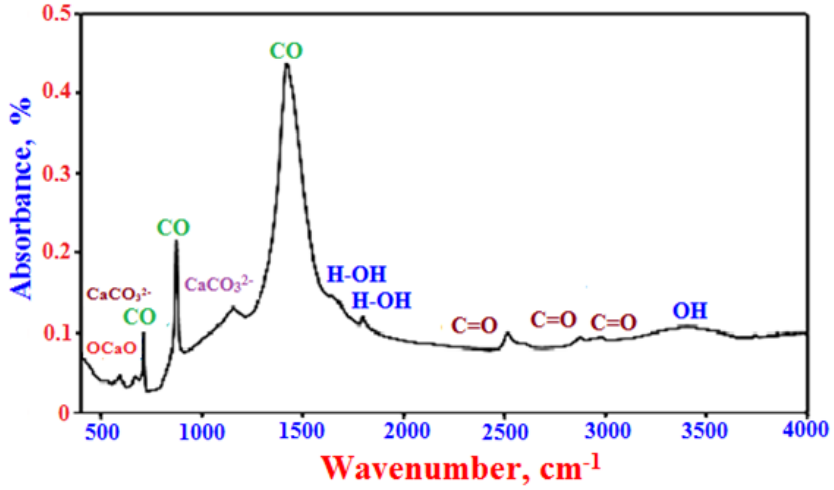

Figure 5: FT-IR spectrum of the eggshell powder.

Physical properties

Water absorption: Water absorption of the various geopolymer bricks incorporated gradual ratios of ES and CCC wastes is graphically represented in Figure 6. It is obvious that the water absorption values of the prepared bricks decreased as the content of

both Egg Shell (ES) and Commercial Calcium Carbonate (CCC) increased up to 12wt. % from each. This means that the apparent porosity of the samples decreased too. With any further increase of either FS or CCC, the water absorption values began to increase. This means that the apparent porosity started to increase, and therefor the mechanical propertied were adversely affected [54,62,66].

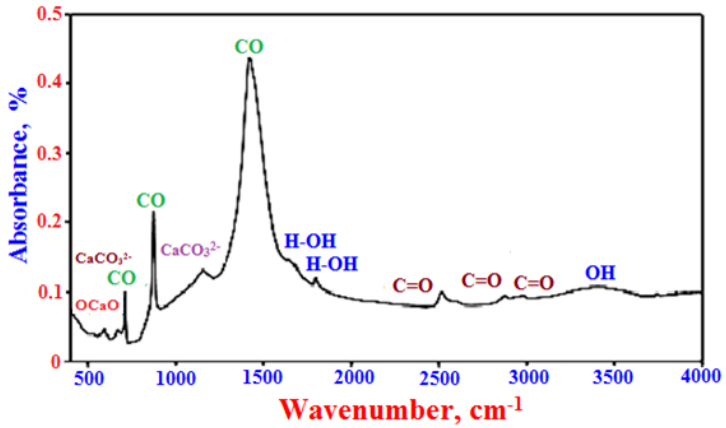

Figure 6: Water absorption of the geopolymer cements containing Egg Shell (ES) and Commercial Calcium Carbonates (CCC).

Apparent porosity: The apparent porosity of the various geopolymer bricks incorporated gradual ratios of ESP and CCC wastes is graphically plotted in Figure 7. It is clear that the apparent porosity results of the prepared bricks decreased with the increase of the contents of both Eggshell Powder (ESP) and Commercial Calcium Carbonate (CCC) up till 12wt. % from each. This means that the water absorption of the brick samples diminished. With any further increase of either FS or CCC contents >12wt. %, the values of apparent porosity started to increase. This means that the water absorption increased too, i.e. results of apparent porosity was conformed with of the water absorption [46,47,66].

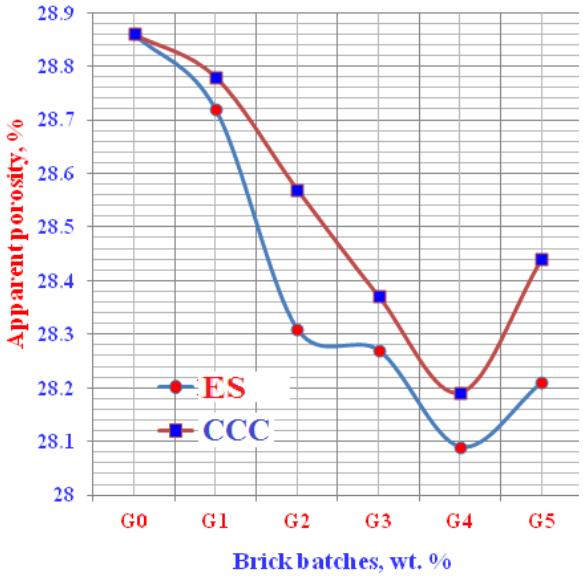

Figure 7: Apparent porosity of the geopolymer cements containing Egg Shell (ES) and Commercial Calcium Carbonates (CCC).

Bulk density: Figure 8 shows the bulk density of the various geopolymer bricks incorporated gradual ratios of ES and CCC wastes. It is obvious that the bulk density data of the prepared bricks improved and enhanced as the content of both Egg Shells (ES) and Commercial Calcium Carbonate (CCC) increased up to 12wt. % from each. This certainly attributed to the decrease of the total porosity of the samples [47,62,66]. With any further increase of either FS or CCC >12wt. %, the obtained data of the bulk density decreased. This may be due to the increase of the total porosity [66-68]. Therefore, the optimum brick batch is that containing about 12wt. % (G4) because it achieved the best results, though that the obtained data with brick batches including the egg shells were higher than those with the commercial carbonates. Hence, the higher quantities from both egg shells and/or commercial carbonates must be avoided.

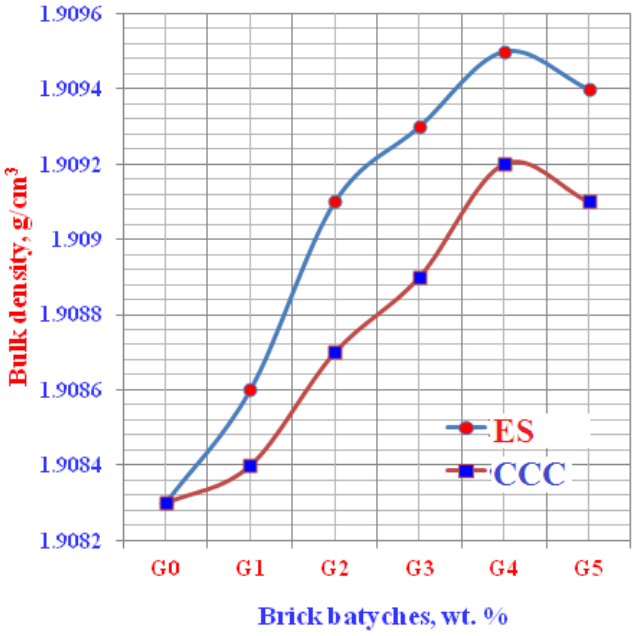

Figure 8: Bulk density of the geopolymer cements containing Egg Shell (ES) and Commercial Calcium Carbonates (CCC).

Mechanical properties

Flexural strength: The flexural strength of the various geopolymer cements incorporated gradual ratios of ES and CCC wastes is graphically drawn in Figure 9. The flexural strength results of the prepared bricks improved and increased as the contents of either egg shells (ES) or Commercial Calcium Carbonate (CCC) increased only up to 12wt. % from each, and then declined. The increase of flexural strength is essentially attributed to the decrease of the total porosity which in turn reflected positively on the bulk density. The improvement and the increase of the bulk density evidently improved and enhanced the flexural strength [62]. The increase flexural strength due to of eggshell powders is mainly contributed to the formation of a large quantity of crystalline phases in the microstructures of geopolymer bricks which could played a vital role in the reaction process between the different components of either ES or CCC [62,66-68]. This also may be acted as filler [68]. However, the obtained flexural strength date with ES was higher than those obtained with CCC. This may be due to the weak reactivity of CCC particles causing a precipitation reaction between the dissolved species during the depolymerization of CCC that is favoring the formation of crystalline phases which can consume a large quantity of the PO_4^{3-} ions from phosphoric acid [67-69]. On the other side, the flexural strength diminished if the content of either ES or CCC increased >12wt. %. Therefore, the higher amounts of both must be prevented.

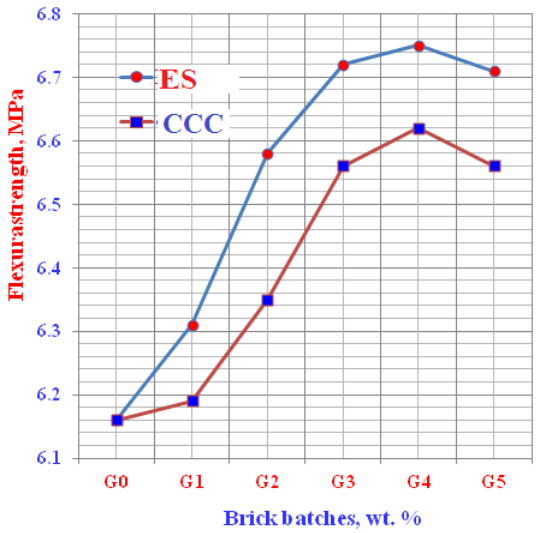

Figure 9: Flexural strength of the geopolymer cements containing Egg Shell (ES) and Commercial Calcium Carbonates (CCC).

Compressive strength: The compressive strength of the prepared geopolymer bricks containing gradual replacing of ES and CCC wastes (0-15wt. %) is graphically plotted in Figure 10. The results of compressive strength of the prepared bricks improved and enhanced with increasing the contents of either Egg Shells (ES) or Commercial Calcium Carbonate (CCC) only up to 12wt. %, and then diminished. The increase of compressive strength is principally attributed to the decrease in the total porosity of the specimens, which in turn reflected positively on the bulk density. Improving of the bulk density evidently improved and enhanced the compressive strength [47,62,68,69]. The increase of compressive strength due to of ES or CCC powders is mainly according to the formation of a large quantity of crystalline phases in the microstructures of geopolymer bricks. This could be played a vital role in the reaction process among the various ingredients of both ES and CCC [66,69]. This also may be due to the filler action of the very fine particles of both [70]. The obtained values of compressive strength with ES were higher than those obtained with CCC. This is mostly due to the weak reactivity of CCC particles than those of ES causing a precipitation reaction between the dissolved species during the depolymerization of CCC. This is favoring the formation of crystalline phases which can consume a large quantity of the PO_4^{3-} ions from phosphoric acid [62,65-70]. On the other hand, the compressive strength diminished when the content of either ES or CCC increased >12wt. %. Therefore, the higher amounts of both wastes must be prevented because the higher amounts of ESP help to create more pores, which in turn reflected negatively on the bulk density and mechanical properties.

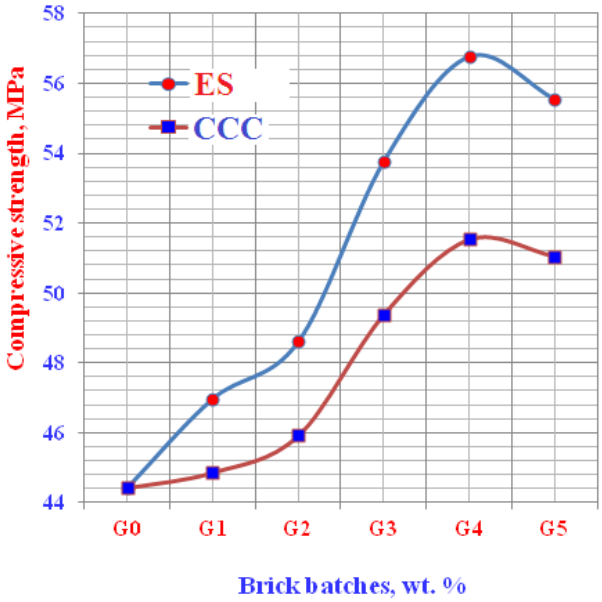

Figure 10: Compressive strength of the geopolymer cements containing Egg Shell (ES) and Commercial Calcium Carbonates (CCC).

General Discussion

When the used T-clay sample was subjected to calcination at the temperature range 0-1000 **°C**, the kaolinite phase (Al_2O_3. $2SiO_2$.$2H_2O$ or AS_2H2) was converted to metakaolin phase (Al_2O_3. $2SiO_2$ or AS_2) through the dissociation of water from its structure at the temperature range 500-600 **°C** (Equation 6). So, the used T-clay was in the form of metakaolin. This phase was in turn converted to mullite phase ($3Al_2O_3$.$2SiO_2$ or A_3S_2) at the temperature range 980 -1000 °C [62,63] as follows:-

$$Al_2O_3.2SiO_2.H_2O \xrightarrow{500-600^\circ C} Al_2O_3.2SiO_2+H_2O \quad (6)$$

$$Al_2O_3.2SiO_2 \xrightarrow{900-1000^\circ C} 3Al_2O_3.2SiO_2 \quad (7)$$

At the temperature range 800-900 **°C**, the limestone or calcium carbonate was decomposed to calcium oxide as follows:

$$CaCO_3 \xrightarrow{800-900^\circ C} CaO+CO_2 \uparrow \quad (8)$$

The formed new phases had interacted with those of ESP and CCC to produce new crystalline phases which improved the physical properties and increased the mechanical properties of the hardened geopolymer cement pastes. On this basis, the density of geopolymer cements increased due to the aluminosilicate materials of metakaolin phase of T-clay. The decrease of the density and the increase of water absorption and porosity are due to the ion size of the pores in geopolymeric cement structures, and the diameters of the pores could be increased as more eggshell powders were added. Although these values decrease, the values of the bulk densities of the geopolymer cements synthesized are much higher than those obtained by other researchers [64,71].

Conclusion

Results demonstrated that both water absorption and apparent porosity decreased with the gradual replacement by ESP or CCC at the expense of the T-C by ratios from both materials by 0, 3, 6, 9, 12

and 15wt. % only up till 12wt. %, while the bulk density increased. The flexural strength and compressive strengths of the prepared geopolymer cements are also improved and enhanced. However, all the characteristics of geopolymer cements based on ESP are higher than those based on CCC. The optimum geopolymer cement was that incorporated 12wt. % ESP waste (G4) because it achieved the best results. It was also concluded that the low-grade calcium carbonate-rich wastes (Egg Shells) can be used to produce porous geopolymer cements. Results also proved that eggshell powder can be used as a pore-creating agent when used with higher quantities when the target is to produce porous geopolymer cements. These types of cements can be used as a thermal insulator material. Moreover, the properties of these porous geopolymer cements could be improved if the concentration of the used solution of phosphoric acid increased.

Acknowledgement

The author wishes to express his deep thanks for National Research Centre for helping to obtain materials, processing, preparing, molding and measuring all of the obtained data of the study.

References

1. Davidovits J (2011) Geopolymer chemistry and applications. (5th edn), Geopolymer Institute, Saint-Quentin, France, p. 612.
2. Arioz E, Arioz O, Kockar OM (2020) Geopolymer synthesis with low sodium hydroxide concentration. Iran J Sci Technol Trans Civ Eng 44: 525-533.
3. Bohra V, Nerella R, Madduru S, Rohith P (2020) Microstructural characterization of fly ash based geopolymer. Mater Today Proc 27: 1625-1629.
4. Cao H, Zhang L, Zheng H, Wang Z (2010) Hydroxyapatite nanocrystals for biomedical applications. The Journal of Physical Chemistry C 114: 18352-18357.
5. Tchakouté KH, Rüscher CH, Kamseu E, Djobo JNY, Leonelli C (2017) The influence of gibbsite in kaolin and the formation of berlinite on the properties of métakaolin phosphate-based geopolymer cements. Materials Chemistry and Physics, p. 199.
6. Zhang ZH, Zhu HJ, Zhou CH, Wang H (2015) Geopolymer from kaolin in China: An overview. Applied Clay Science 119: 31-41.
7. Ge Y, Yuan Y, Wangliu K, He Y, Cui X (2015) **Preparation of geopolymer-based inorganic membrane for removing Ni^{2+}** from wastewater. Journal of Hazardous Materials 299: 711-718.
8. Bai C, Franchin G, Elsayed H, Zaggia A, Conte L, et al. (2017) High-porosity geopolymer foams with tailored porosity for thermal insulation and wastewater treatment. Journal of Materials Research 32: 3251-3259.
9. Strini A, Roviello G, Ricciotti L, Ferone C, Messina F, et al. (2016) TiO_2 -based photocatalytic geopolymers for nitric oxide degradation. Materials 9: 513.
10. Singh B; Rahman MR, Paswan R, Bhattacharyya SK (2016) Effect of activator concentration on the strength, ITZ and drying shrinkage of fly ash/slag geopolymer concrete. Constr Build Mater 118: 171-179.
11. Kumar EM, Ramamurthy K (2017) Influence of production on the strength, density and water absorption of aerated geopolymer paste and mortar using Class F fly-ash. Construction and Buildings Materials 156: 1137-1149.
12. Kamseu E, Nait-Ali B, Bignozzi MC, Leonelli C, Rossignol S, et al. (2012) Bulk composition and microstructure dependence of effective thermal conductivity of porous inorganic polymer cements. Journal of the European Ceramic Society 32: 1593-1603.
13. Font A, Borrachero MV, Soriano L, Monzó José, Payá J (2017) Geopolymer eco-cellular (GECC) based on fluid catalytic cracking catalyst residue (FCC) with addition of recycled aluminum foil powder. Journal of Cleaner Production 168: 1120-1131.
14. Luna-Galiano Y, Leiva C, Arenas C, Fernandez-Pereira C (2018) Fly ash-based geopolymeric foams using silica fume as pore generation agent. Physical, mechanical and acoustic properties. Journal of Non-Crystalline Solids 500: 196-204.
15. Novais RM, Buruberri LH, Ascensao G, Seabra MP, Labrincha JA (2016) Porous biomass fly ash-based geopolymers with tailored thermal conductivity. Journal of Cleaner Production 119: 99-107.
16. Cilla MS, Morelli MR, Colombo P (2014) Open cell geopolymer foams by a novel saponification / peroxide / gel casting combined route. Journal of the European Ceramic Society 34: 3133-3137.
17. Vaou V, Panias D (2010) Thermal insulating foamy geopolymers from perlite. Minerals Engineering 23: 1146-1151.
18. Abdollahnejad Z, Pacheco-Torgal F, Félix T, Tahri W, Aguiar JB (2015) Mix design, properties and cost analysis of fly ash-based geopolymer foam. Construction and Building Materials 80: 18-30.
19. Tchakouté KH, Elimbi A, Yanne E, Djangang CN (2013) Utilization of volcanic ash for the production of geopolymers cured at ambient temperature. Cement and Concrete Composites 38: 78-81.
20. Darweesh HHM, Abo El-Suoud MR (2014) Setting, hardening and mechanical properties of some cement / agrowaste composites - part I. American Journal of Mining and Metallurgy 2(2): 32-40.
21. Darweesh HHM (2020) Specific characteristics and microstructure of Portland cement pastes containing wheat straw ash (WSA) Indian Journal of Engineering 17(48): 569-583.
22. Darweesh HHM (2020) Influence of Sunflower Stalk Ash (SFSA) on the behavior of Portland cement paste. Results in Engineering 8: 100171.
23. Darweesh HHM, Abo El-Suoud MR (2019) Influence of sugarcane bagasse ash on Portland cement characteristics. Indian J of Engineering 16: 252-266.
24. Darweesh HHM, Abo El-Suoud MR (2017) Saw dust ash substitution for cement pastes-Part I. American J of Construction and Building Materials 2(1): 1-9.
25. Darweesh HHM (2021) Characterization of coir pith ash blended cement pastes. Research & Development in Material science 15(1): 1630-1639.
26. Darweesh HHM (2021) Utilization of physalis pith ash as a pozzolanic material in portland cement pastes. Journal of Biomaterials 5(1): 1-9.
27. Darweesh HHM (2019) Recycling of glass waste in ceramics- Part I: physical, mechanical and thermal characteristics. Springer Nature Applied Sciences 1: 1274-1280.
28. Darweesh HHM, Abo El-Anwar A, Mekky HM (2018) Addition of limestone at the expense of gypsum in portland cement. Interceram International Ceramic Review 67(5): 18-26.
29. Zhang Z, Provis JL, Reid A, Wang H (2015) Mechanical, thermal insulation, thermal resistance and acoustic absorption properties of geopolymer foam concrete. Cement and Concrete Composites 62: 97-105.
30. Ngouloure ZNM, Nait-Ali B, Zekeng S, Kamseu E, Melo UC, et al. (2015) Recycled natural wastes in metakaolin-based porous geopolymers for insulating applications. Journal of Building Engineering 3: 58-69.
31. Bell JL, Kriven WM (2009) Preparation of ceramic foams from metakaolin-based geopolymer gels. Ceramics Engineering Science Procedure 29: 97-111.
32. Shiu HS, Lin KL, Chao SJ, Hwang CL, Cheng TW (2014) Effects of foam agent on characteristics of thin-film transistor liquid crystal display

waste glass-metakaolin-based cellular geopolymer. Environmental Progress Sustainable Energy 33: 538-550.

33. Landi E, Medric V, Papa E, Dedecek J, Klein P, et al. (2013) Alkali-banded ceramics tailored porosity. Applied Clay Science 73: 56-64.

34. Sasmal N, Garai M, Karmakar B (2015) Preparation and characterization of novel foamed porous glass ceramics. Materials Characterization 103: 90-100.

35. Fernandes HR, Ferreira DD, Andreola F, Lancellotti I, Barbieri L, et al. (2014) Environmental friendly management of CRT glass by foaming with waste egg shells, calcite or dolomite. Ceramics International 40: 13371-13379.

36. Alghamdi H, Neithalath N (2018) Novel synthesis of lightweight geopolymer matrices from fly ash through carbonate-based activation. Materials Today Communications 17: 266-267.

37. Issawy B (1981) Geology of the southwestern desert of Egypt. Ann Geol Surv Egypt 11: 57-66.

38. Issawy B (1996) The geology of Kurkur Dungul area. Geol Surv Egypt 46: 102.

39. Ahmed SM (2003) Geomorphic evolution and sediment ion of the Tufa and Travertine deposits in Kurkur area, southwestern Desert, Egypt. Egypt J Geol 40(1): 119-140.

40. Awad HM (2003) Geological and ceramic studies on some shale deposits around Tushka area, south valley, Egypt. PhD Thesis, Fac Sci Cairo Univ, Egypt.

41. Darweesh HHM (2012) Densification and thermomechanical properties of conventional ceramic composites containing two different industrial byproducts. American-Eurasian Journal of Scientific Research 7(3): 123-130.

42. Wagh AS (2005) Chemistry bonded phosphate ceramics - a novel class of geopolymers. **Ceramics Transactions 165**: 1007-116.

43. Bai C, Franchin G, Elsayed H, Zaggia A, Conte L, et al. (2017) High-porosity geopolymer foams with tailored porosity for thermal insulation and waste-water treatment. Journal of Materials Research 32: 3251-3259.

44. Landi E, Medric V, Papa E, Dedecek J, Klein P, et al. (2013) Alkali-banded ceramics tailored porosity. Applied Clay Science 73: 56-64.

45. Sasmal N, Garai M, Karmakar B (2015) Preparation and characterization of novel foamed porous glass ceramics. Materials Characterization 103: 90-100.

46. Fernandes HR, Ferreira DD, Andreola F, Lancellotti I, Barbieri L, et al. (2014) Environmental friendly management of CRT glass by foaming with waste egg shells, calcite or dolomite. Ceramics International 40: 13371-13379.

47. Darweesh HHM, Abo El-Suoud MR (2019) Palm ash as a pozzolanic material for portland cement pastes. To Chemistry Journal 4: 72-85.

48. Darweesh HHM (2012) Setting, hardening and strength properties of cement pastes with zeolite alone or in combination with slag. Interceram International 1: 52-57.

49. Darweesh HHM (2021) Light-weight bricks from clay combined with cement kiln dust and sludge wastes. Intern J Res in Eng 3(1): 12-18.

50. Kishar EA, Ahmed DA, Kassem NN (2018) Geopolymer cement based on alkali activated slag-part 1. JSRS 34: 538-552.

51. Giergiczny Z (2019) Fly ash and slag. Cem Concr Res 124: 105826.

52. ASTM Standards C348 (2018) Standard test method for flexural strength of hydraulic-cement mortars. ASTM: West Conshohocken, PA, USA.

53. Hewlett PC, Liska M (2017) Lea's chemistry of cement and concrete, (5th edn), Edward Arnold Ltd., London, England.

54. Darweesh HHM, Aboel-Suoud MR (2020) Effect of agricultural waste material on the properties of portland cement pastes. Journal of Research & Development in Material science 13(1): 1360-1367.

55. ASTM- C170-90 (1993) Standard test method for compressive strength of dimension stone. Pp. 828-830.

56. ASTM-C109M (2013) Standard test method for compressive strength of hydraulic cement mortars (Using 2-in. Or [50-mm] Cube Specimens), Annual Book of ASTM Standards. ASTM International, West Conshohocken, PA.

57. Darweesh HHM (2017) Geopolymer cements from slag, fly ash and silica fume activated with sodium hydroxide and water glass. Interceram International 6(1): 226-231.

58. Garrett TD, Cardenas HE, Lynam JG (2020) Sugarcane bagasse and rice husk ash pozzolans: Cement strength and corrosion effects when using saltwater. Current Research in Green and Sustainable Chemistry 1-2: 7-13.

59. Myers RJ, L'Hôpital E, Provis JL, Lothenbach B (2015) Composition-solubility-structure relationships in calcium (alkali) aluminosilicate hydrate (C-(N,K-)A-S-H). Dalton Trans 44(30): 13530-13544.

60. Darweesh HHM (2020) Characteristics of Portland cement pastes blended with silica nanoparticles. To Chemistry 5.

61. Darweesh HHM (2020) Recycling of glass waste in ceramics-part II: Microstructure of ceramic products using XRD, DTA and SEM techniques. Research & Development in Material science 13(4): 1424-1431.

62. Anjaneyulu U, Sasikumar S (2014) Bioactive nanocrystalline wollastonite synthesized by sol-gel combustion using eggshell waste as calcium source. Bulletin of Materials Science 37: 207-212.

63. Hongxia G, Zhenping Q, Peng Q, Peng Y, Suping C, et al. (2011) Crystallization of aragonite $CaCO_3$ with complex structures. Advances Powder Technology 22: 777-783.

64. Choudhary R, Koppala S, Swamiappan S (2015) Bioactivity studies of calcium magnesium silicate prepared from eggshell waste by sol-gel combustion synthesis. Journal of Asian Ceramic Society 3: 173-177.

65. Darweesh HHM (2001) Building materials from siliceous clay and low-grade dolomite rocks. Ceramics International 27: 45-50.

66. Hassan HS, Abdel-Gawwad HA, V**á**squez Garc**í**a SR, Israde-Alc**á**ntara I (2018) Fabrication and characterization of thermally-insulating coconut ash-based geopolymer foam. Waste Management 80: 235-240.

67. Riyap HI, Bewa CN, Banenzou**é** C, Tchakouté HK, R**ü**scher CH, et al. **(2019) Microstucture and mechanical,** physical and structural properties of sustainable lightweight metakaolin-based geopolymer cements and mortars employing rice husk. Journal of Asian Ceramic Societies 7: 199-212.

68. Darweesh HHM (2020) Metakaolin blended cement pastes. International Journal of Innovative Studies in Sciences and Engineering Technology (IJISSET) 6(1): 5-18.

69. Alghamdi H, Neithalath N (2018) Novel synthesis of lightweight geopolymer matrices from fly ash through carbonate-based activation. Materials Today Communications 17: 266-267.

70. Wongsa A, Sata V, Nematollahi B, Sanjayan J, Chindaprasirt **P (2018)** Mechanical and thermal properties of lightweight geopolymer mortar incorporating crumb rubber. Journal of Cleaner Production 195: 1069-1080.

71. Fongang RTT, Pemndje J, Lemougna PN, Melo UC, Nanseu CP, et al. (2015) Cleaner production of the lightweight insulating composites Microstructure, pore network and thermal conductivity. Energy and Building 107: 113-122.